PII: S0032-3861(97)10350-0

Polymer Vol. 39 No. 21, pp. 5147–5153, 1998
0032-3861/98/$ – see front matter

Influence of processing conditions on the multiphase structure of segmented polyurethane

G. Pompe*, A. Pohlers, P. Pötschke and J. Pionteck
Institute of Polymer Research Dresden, P.O. Box 120411, Dresden, Germany
(Received 4 June 1997; revised 12 September 1997; accepted 25 November 1997)

The multiphase structure of thermoplastic polyurethane elastomers is not only influenced by the chemical structure, but also by the processing conditions. The polymorphism of hard segment (HS) crystallites of a commercial polyurethane was investigated in dependence on the melt processing conditions using WAXS and d.s.c. The observed crystalline morphology types are strongly influenced by the processing temperature. Analysis of the results permits the assignment of HS crystallites of so-called 'type II' with high WAXS intensity to those melting above 220°C. Additionally, the tensile strength was determined. These results related to the d.s.c. data allow to establish a processing–structure–property relation. © 1998 Elsevier Science Ltd. All rights reserved.

(Keywords: polyurethane; processing conditions; polymorphism of hard segment crystallites)

INTRODUCTION

Thermoplastic polyurethane elastomers (TPU) are linear multiblock copolymers containing soft and hard segments. The hard segments (HS) are based on diisocyanates and a low-molecular weight diol and/or diamine. The soft segments (SS) consist either of polyether or polyester glycols, which may be extended by diisocyanates. Thermodynamic immiscibility[1] of hard and soft segments at low temperature results in phase separation and, consequently, in a domain structure. This multiphase structure first proposed by Cooper and Tobolsky[2] is the reason for the extraordinary properties of segmented polyurethanes. The glassy or semicrystalline HS domains act as physical crosslinks and reinforcing fillers, while the SS phase causes the flexibility of these elastomers. Normally, the phase separation is incomplete and the hard and soft segment phases still contain a certain amount of the other segments[3–5].

There is a large number of possible polyurethanes varying in structure of the monomers, in composition and, therefore, in properties. Due to the economic importance of TPU based on 4,4′-diphenylmethanediisocyanate (MDI), 1,4-butanediol (BD), and a polyether or a polyester macroglycol, the research efforts have been focused on this particular class of thermoplastic polyurethane elastomers. The final properties of the TPU are determined not only by the chemical structure and composition, but also by the synthesis conditions and thermal history. It is generally assumed that changes in the thermal history result in a different microphase structure of the TPU[6,7].

With increasing temperature the amorphous HS dissolve in the soft segments[5,8]. This process is very fast above the melting temperature of the HS crystallites, and the melt becomes homogeneous[8,9]. During cooling from the melt the phase separation starts again. Since the mobility of the polymer chains decreases with decreasing temperature, the phase separation process will be hindered. In dependence on the cooling and postannealing conditions, different domain and crystallite morphologies as well as varying degrees of phase separation[5,10–14] are possible. A very long annealing time at room temperature, or a postannealing at temperatures near or above the glass temperature of the hard segments[5,8], are necessary to approach an equilibrium state.

The hard segment microdomains show a more or less ordered state which can be analysed by wide-angle X-ray scattering (WAXS) and differential scanning calorimetry (d.s.c.). The multiple melting behaviour of MDI-diol-based polyurethanes obtained by d.s.c. investigations is intensely discussed in the literature[3,6,9,10]. In general, one can observe two temperature ranges of endothermic behaviour at about 170°C and from 190 to 230°C. The low temperature range (as well as the small endothermic range at about 80°C[6,16]) is considered to be caused by disordering of HS crystallites with relatively short-range order, and the endothermic peaks at higher temperatures are related to HS crystallites with long-range order[6,15,16].

A first proposal for the crystal structure of MDI-BD hard segments was given by Bonart *et al.*[10]. Blackwell and coworkers[11,12] investigated different states of MDI-BD-based polyurethanes and found two distinct morphologies of the HS crystallites, the so-called 'extended' and 'contracted' forms. The existence of two different morphologies was confirmed by other authors[13,15]. Briber and Thomas[13] introduced the indication 'type I' and 'type II' which will be used in this paper. The appearance of the polymorphism strongly depends on the thermal history and annealing conditions. It should be mentioned that a further morphology ('type III') can be observed at specimens stretched at about 100°C[17]. The multiple melting behaviour should be explained by both the polymorphism and reorganisation of HS crystallites during heating in d.s.c. An excellent review concerning the multiple melting and the polymorphism observed in TPU is given by Koberstein and Galambos[15]. Not only the existence and the content of different HS

* To whom correspondence should be addressed

Table 1 Overview of investigated samples

Sample	Preparation conditions and/or maximum processing temperature	Shape of sample
(a) V	Virgin granules (commercial product)	Granules
(b) E	Virgin granules V extruded at 240°C	Granules
(c)	Injection moulding of virgin granules V	Dumbbells S3 and bars for DMA
V210	210°C	Dumbbells S3 and bars for DMA
V240[a]	240°C	Dumbbells S3 and bars for DMA
(d)	Injection moulding of extruded granules E	Dumbbells S3 and bars for DMA
E210	210°C	Dumbbells S3 and bars for DMA
E220	220°C	Dumbbells S3 and bars for DMA
E230	230°C	Dumbbells S3 and bars for DMA
E240	240°C	Dumbbells S3 and bars for DMA
(e) R230	Thermal treatment of virgin granules V in a rheometer for 30 mn at 230°C	Foil

Samples b, c, d were postannealed for 24 h at 100°C
[a]Mould temperature = 60°C

morphologies strongly depend on the preparation conditions and on the thermal history, but also the degree of phase separation and the overall TPU morphology. In this way the processing–structure–property relationship is very complex. Li *et al.*[5] pointed out that all parameters, including thermal and mechanical history, thermal transitions, or the condition of the thermal characterisation, need to be designed carefully for an unambiguous interpretation and discussion of the results.

In the present paper WAXS and d.s.c. studies were carried out on one (chemically identical) polyurethane based on MDI, BD, and polyesterdiol. The melting behaviour and the morphology of the HS were investigated in dependence on the processing type and processing temperatures. Additionally, mechanical properties were determined and discussed in relation to the results of the WAXS and d.s.c. studies.

EXPERIMENTAL

Material and processing

The thermoplastic polyurethane used is a linear block copolymer based on polyethylene adipatediol, 1,4-butanediol (BD), and 4,4′-diphenylmethanediisocyanate (MDI), with a hard segment content of about 60 wt% and a shore D hardness of 60 (Elastogran, Germany). Before processing the granules were dried in vacuum for 3 h at 100°C.

The TPU was extruded by use of a co-rotating, intermeshing twin-screw extruder ZSK 30 (L/D = 32, Werner and Pfleiderer, Germany) with a screw configuration adapted to TPU. The screw speed was 150 r.p.m., the output 10 kg/h. The maximum melt temperature was 240°C, the residence time was about 50 s. The strands were cooled in a water bath (about 25°C), and the pelletizing was subsequently carried out. A Battenfeld 500/200 machine (Battenfeld, Germany) was applied for injection moulding. The residence time in the molten state was up to 5 min at the selected maximum melt temperature. The injection pressure was about 70 bar, and the cycle time 30 s. The melt temperature was varied. The mould temperature was 30°C. Specimens S3 following DIN 53455 for the tensile test and bars for DMA were produced with the same mould. The number in the sample indication (see *Table 1*) is the adjusted highest temperature during injection moulding. Bars were prepared from both virgin granules V (V2XX) and extruded granules E (E2XX). The specimens were tested after annealing for 24 h at 100°C.

In addition, one sample (R230) was prepared by annealing of virgin granules in an RMS 800 rheometer (Rheometrics, Germany) in N_2 atmosphere, using a plate–plate geometry. The sample was thermally treated at 230°C for 30 min at the same conditions as used for measuring the viscosity (frequency = 100 rad/s, strain = 10%, tact = 15 s). Afterwards, the sample was slowly cooled and stored at room temperature.

Wide angle X-ray scattering (WAXS)

The X-ray patterns were obtained by a four-circle diffractometer using the HiStar area detector (AXS, Germany) and Kα-monochrome Cu-radiation (40 kV/30 mA). WAXS measurements were carried out at room temperature by a symmetric transmission procedure. In the case of injection moulded specimens the sample was taken out of the centre of the bars and investigated perpendicular to the injection direction. Data were obtained with a radial scan 2Θ from 5 to 40° using the GADDS software (AXS, Germany). These data were analysed with the APX 63 software (FPM-Seifert, Germany) in connection with a self-developed module, DIFF2. Background and amorphous part were separated by a regression procedure.

Differential scanning calorimetry (d.s.c.)

The d.s.c. measurements were realised with a DSC7 (Perkin-Elmer, USA) in a temperature range from − 60 to +280°C. In the case of injection moulded specimens the sample (≈ 8 mg) was taken out of the centre of the bars. The influence of a possible reorganisation during the heating scan was suppressed using a heating rate of 40 K/min[9,15]. In this way, the observed melting behaviour presents more or less the state of crystalline morphology at room temperature after the processing. The high heating rate is necessary to correlate the results of d.s.c. with those of WAXS and mechanical properties, determined at room temperature.

The temperatures and transition enthalpy were calibrated with In and Pb standards with a heating rate of 10 K/min. The thermal lag of temperatures (about 3 K) caused by the high scan rate was not corrected. All samples were measured under the same conditions.

Dynamic mechanical analysis (d.m.a.)

The determination of the glass transition temperatures was performed using a RMS 800 (Rheometrics, Germany) under torsion rectangular conditions. Injection moulded bars (80 × 10 × 2 mm) were investigated in the temperature

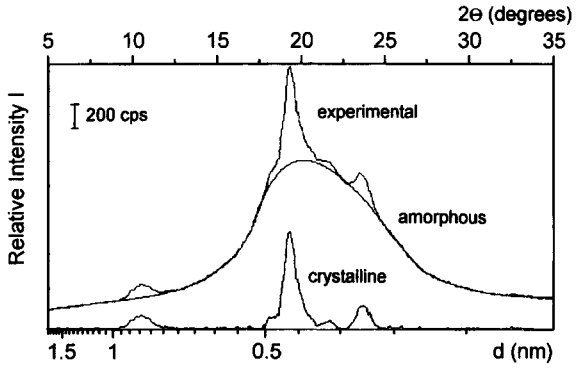

Figure 1 Experimental WAXS curve for sample V and its separation in the amorphous and crystalline parts

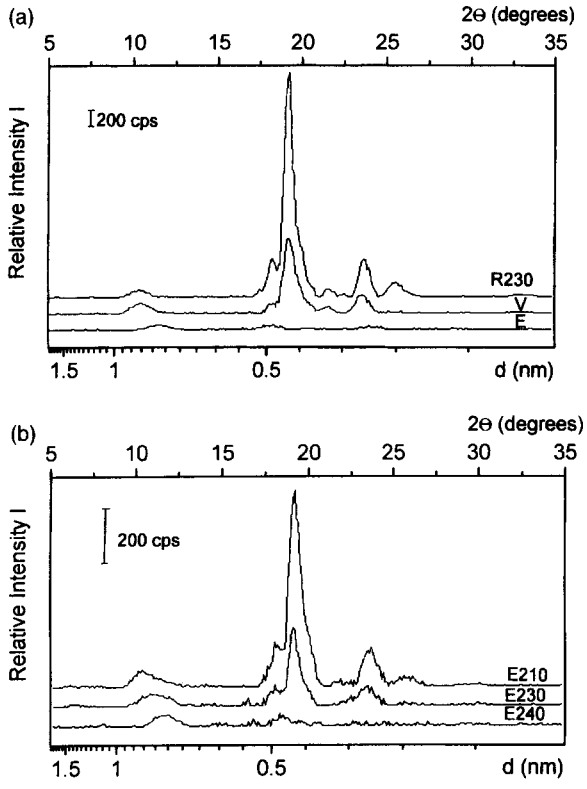

Figure 2 (a) Influence of processing type on the crystalline part of WAXS curves: samples V, E, and R230. (b) Influence of processing temperature during injection moulding on the crystalline part of WAXS curves: samples E210, E230, and E240

range from −100 to +200°C with a heating rate of 5 K/min, a frequency of 10 Hz, and a strain of 0.03–0.5%. The maximum temperature of the tan δ peak is discussed as glass transition temperature.

Mechanical testing

Measurements of tensile properties were carried out at room temperature using a Tira Test machine (Germany) with a long-distance recorder LA800. Dumbbells S3 (DIN 53455) with a gauge length of 50 mm and a speed of 50 mm/min were used. Reported data are the average of 10 measurements.

RESULTS

WAXS

The experimental WAXS results and the separated scatterings of the amorphous and crystalline part are given in *Figure 1* for the virgin granules V. The crystalline scatterings of the samples V, E, and R230 are represented in *Figure 2a*. The influence of the melt temperature during injection moulding on the crystalline scattering is shown in *Figure 2b*.

Table 2 Crystallinity index α_X determined by WAXS (range of integration: $2\Theta = 7–35°$)

Sample	ΣT_{am}	ΣT_{cr}	α_X (%)	$\alpha_{X,I}$ (%)	$\alpha_{X,II}$ (%)
V	12676	1366	9.75 ± 0.5	0.7	9.05
R230	12466	3287	21.0	0.2	20.8
E	12545	245	1.9	0.9	1.0
E210	13392	1010	7.0	0.4	6.6
E230	13458	542	3.9	0.4	3.5
E240	12456	165	1.2	0.5	0.7

The crystallinity index α_X is defined as the ratio of the area under the separate crystalline pattern (ΣT_{cr}) and the total scattering ($\Sigma T_{cr} + \Sigma T_{am}$) of the original pattern:

$$\alpha_X = \Sigma T_{cr} / (\Sigma T_{cr} + \Sigma T_{am}) \quad (1)$$

The areas were obtained by integration between $2\Theta = 7$ and 35°. In *Table 2* the values of α_X are listed. The crystallinity index α_X of the virgin granules and the extruded and injection moulded samples is rather small and in the range from 10 (virgin granule V) to 1% (sample E240). Extrusion of the virgin granules reduces the crystallinity index from 10 to about 2% (sample E). The injection moulding of the extruded granules E at 240°C hardly changes the crystallinity index. At processing temperatures ≤ 230°C the crystallinity index increases with decreasing melt temperature up to about 7% (E210). Sample R230 shows an extremely different behaviour. By the special thermal treatment in the rheometer at 230°C the crystallinity index α_X increases from 10%, observed by the virgin granules V used, to more than 20%.

The intensity of the reflections depends strongly on the thermal history. The *d*-spacings of the observed reflections were determined by peak separation using a Gaussian profile. An overview of the *d*-spacings and their assignments to the types is given by Koberstein and Galambos[15]. The values of some *d*-spacings differ slightly. In *Table 3* the *d*-spacings obtained at R230 are listed. Their assignment to the crystallite types is based on the proposal of Briber and Thomas[13]. Almost all samples show reflections of HS crystallites 'type I' and 'type II'. We assume that the 'type III' does not exist in our samples, since this type is only observed in high oriented solids[17].

According to this assignment (*Table 3*) the scattering parts of 'type I' and 'type II' $\alpha_{X,i}$ can be estimated with

$$\alpha_{X,i} = \alpha_X * \Sigma T_{cr,i} / \Sigma T_{cr} \quad i = \text{type I, II} \quad (2)$$

and

$$\Sigma T_{cr} = \Sigma T_{cr,I} + \Sigma T_{cr,II}. \quad (3)$$

The results are given in *Table 2*. The values of $\alpha_{X,I}$ are very small. Within the limit of error these values are almost equal in all samples. It is remarkable that the crystallinity index of the extruded granules E and the injection moulded sample E240 is nearly the same, indicating that the processing temperature (in both samples 240°C) dominantly influences the crystallite morphology compared to the type of processing. The content $\alpha_{X,II}$ strongly increases with decreasing processing temperature, analogously to the overall crystallinity index α_X.

Table 3 *d*-spacings of crystalline reflections and their assignment to 'type I' and 'type II', analogously to Briber and Thomas[13]

d (nm)			
Type I		Type II	
Own results[a]	Briber and Thomas[13]	Own results[a]	Briber and Thomas[13]
		0.85 (m)	0.86 (m)
0.76 (m)	0.77 (w)		
0.506 (w)	0.501 (s)		
			0.494 (s)
		0.484 (s)	
		0.462 (vs)	0.461 (s)
		0.446 (m)	0.445 (m)
0.435 (w)[b]			
		0.413 (w)	0.416 (m)
0.397 (w)			
	0.389 (m)		
		0.375 (s)	0.381 (m)
0.362 (w)[c]			
	0.353 (w)		
		0.348 (m)	0.351 (w)
		0.337 (w)	

vs, very strong; s, strong; m, medium; w, weak

[a]Exact values from sample R230, the deviation of values of other samples is within the limit of $\pm$ 0.005 nm ($d < 0.6$ nm), $\pm$ 0.007 nm ($d = 0.76$ nm), and $-$ 0.015 nm ($d = 0.85$ nm), respectively

[b]This assignment results from comparison of observed *d*-spacings listed in Table 1 of Koberstein and Galambos[15] (the authors and Born *et al.*[18] found *d*-spacings at 0.425–0.43 nm only in structures which show also *d*-spacings at 0.76 nm characterizing 'type I')

[c]Only identified at the samples E and E240

The crystallinity index α_X is determined mainly by the very strong reflection at $d = 0.461$ nm caused by HS crystallites 'type II'. The HS crystallites 'type I' do not show a reflection with comparable intensity. As Briber and Thomas[13] have already assumed, the HS crystallites 'type I' must be much smaller than those of 'type II', and in this way the WAXS method is insufficient to detect such small HS crystallites quantitatively.

D.s.c.

Figure 3a shows the heating scans of samples V, E, and R230. Strong differences in the melting behaviour were observed. In the virgin granules V the main part of crystallites melts at rather high temperatures (melt peaks at 212 and 231°C), whereas in the extruded granules E (maximum processing temperature, 240°C) the melting range is shifted to lower temperatures. The dominant melt peaks of this sample are at 187 and 212°C.

The treatment of the virgin granules at 230°C for 30 min in the rheometer (R230) represents an excellent annealing. Consequently, a special melting behaviour is observed. Instead of a broad multiple melting range, a sharp peak at 252°C is found, and the heat of fusion increases from 26 up to 35 J/g.

In *Figure 3b* the melting behaviour of the injection moulded samples (E2XX) is compared with the melting behaviour of the extruded granules (sample E). Injection moulding at $T \leq 230$°C causes both recrystallization of the molten and annealing of the non-molten part. Consequently, HS crystallites with melting temperatures T_m above 220°C will be formed during processing. In contrast, the melting behaviour of specimen E240 injection moulded at $T > 230$°C is unchanged compared to granules E. A comparison with the results of Leung and Koberstein[9] is not possible. Their 'annealing' is similar to a crystallization process of a molten state using different conditions. In our case, the dominant effect of the different processing temperature is the change of the molten and non-molten parts of HS crystallites.

In *Table 4* the determined heats of fusion are listed. The heat of fusion was separated in the part ΔH_1 (100–160°C), formed mainly during postannealing of the samples at 100°C, and the part ΔH_2 (160–245°C), formed mainly during processing (*Table 4*). ΔH_1 is slightly different in dependence on the state of morphology formed. ΔH_2 shows only small changes. Its smallest value is found at the processing temperature of 230°C.

The melting temperature region between 160 and 240°C consists of multiple melting peaks. In consequence of the two morphologies of HS crystallites detected by WAXS, the heat of fusion ΔH_2 is separated into two parts $\Delta H_{2,I}$ and $\Delta H_{2,II}$. These parts are calculated by partial integration using 220°C as temperature limit (see *Figure 3a,b*). This temperature limit was estimated from the heating scan of sample V and is used for all samples. Considering this approximation, and in consequence of the thermal effects of high heating rate, the values $\Delta H_{2,I}$ (partially integrated between 160 and 220°C) and $\Delta H_{2,II}$ (partially integrated between 220 and 245°C) can be used only in regard to quality. Since the melting peaks of the samples E220 and E230 overlap strongly, the partially integrated values of these samples give only a coarse approximation.

DISCUSSION OF THE RESULTS OF WAXS AND D.S.C.

The heat of fusion ΔH_2 is used as a measure of the overall crystallinity determined by d.s.c., and α_X as the overall crystallinity determined by WAXS. In *Figure 4* the heat of fusion ΔH_2 is plotted in dependence on the crystallinity index α_X for all investigated samples. It can be observed that the heat of fusion ΔH_2 is about constant in spite of strong changes of α_X. Only the sample R230 shows a higher value of the heat of fusion than the other samples.

To understand this behaviour, the indices of crystallinity α_X, $\alpha_{X,I}$, and $\alpha_{X,II}$ and the values of ΔH_2, $\Delta H_{2,I}$, and $\Delta H_{2,II}$ are plotted in dependence on the processing temperature in *Figure 5a,b*. Additionally, the values of the granules V and E are represented. The values of the crystallinity indices α_X and $\alpha_{X,II}$ are about the same. This means, α_X will be mainly determined by $\alpha_{X,II}$. In the case of injection moulding of granules E, both indices increase strongly with decreasing processing temperature. In contrast to this result, the index of crystallinity $\alpha_{X,I}$ caused by HS crystallites 'type I' is much smaller and almost constant.

It is interesting that the behaviour of $\Delta H_{2,II}$ (*Figure 5b*) corresponds to that of $\alpha_{X,II}$. However, as opposed to the results obtained by WAXS the melting heat ΔH_2 used as the measure for the overall crystallinity is hardly changed, and $\Delta H_{2,I}$ increases with increasing processing temperature.

The comparison of the results obtained by WAXS and d.s.c. shows that the HS crystallites 'type II' are apparently the same crystallites which melt at $T > 220$°C. These crystallites have obviously a large size and/or a high order and determine mainly α_X.

The sample R230 shows the highest crystallinity with both methods (*Figure 4*). It is interesting that in this sample only crystallites of 'type II' were detected by WAXS. The thermal treatment of this sample results apparently in an increase of size and perfection of HS crystallites 'type II'.

The values α_X, $\alpha_{X,II}$, and $\Delta H_{2,II}$ of all investigated samples were related to the values α_X(R230) ($= \alpha_{X,II}$(R230)) and ΔH_2(R230), respectively. This calculation is based on the

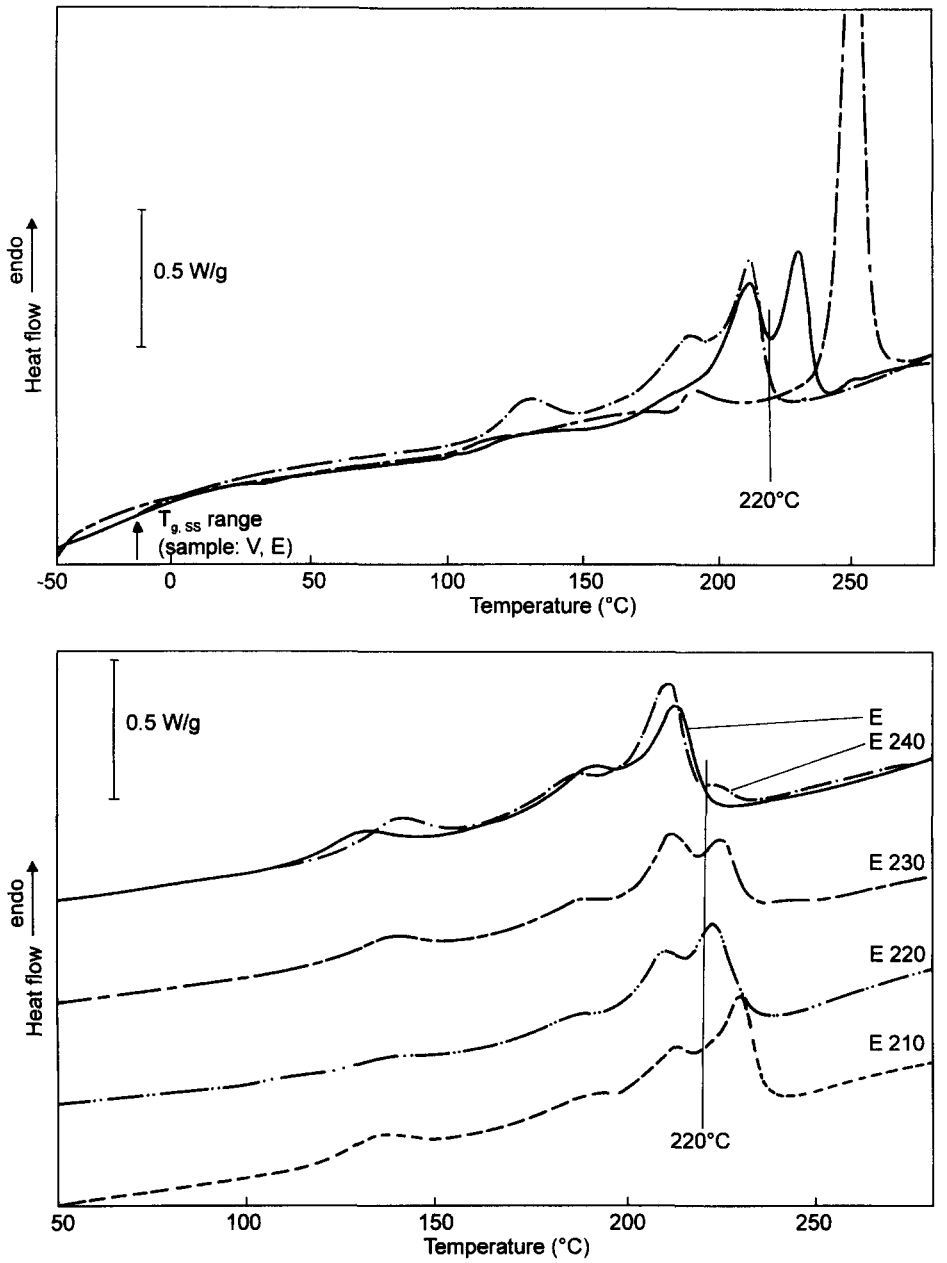

Figure 3 (*a*) Influence of processing type on d.s.c. heating curves: samples V, E, and R230 (heating rate, 40 K/min). (*b*) Influence of processing temperature during injection moulding on the melting range of d.s.c. heating curves: samples E210–E240 (heating rate, 40 K/min)

Table 4 Heats of fusion of HS crystallites determined by d.s.c.

Sample	ΔH (J/g) (100°C–T_2)[a]	ΔH_1 (J/g)	ΔH_2 (J/g)	$\Delta H_{2,I}$ (J/g)	$\Delta H_{2,II}$ (J/g)
V	26.4	1.8	24.4	15.1	9.3
V210	30.6	4.7	25.9	≥ 13.6	≤ 16.5
	(T_2 = 255°C)				
V240	32.8	6.2	24.9	23.2	3.6
E	28.7	5.9	22.8	22.5	0.3
	(T_2 = 230°C)				
E210	28.6	4.6	24.0	14.8	9.2
E220	25.1	2.8	22.2	15.9	6.3
E230	23.9	2.9	20.4	15.3	5.1
E240	31.3	6.7	24.6	≈ 23.6	≈ 1.0
	(T_2 = 235°C)				
R230	35.4	2.2			
	(T_2 = 275°C)	3.3[b]	32.5[b]	1.2[b]	30.9[b]

[a]If no comment, then T_2 = 245°C
[b]Upper and/or lower limit of integration: 185 instead of 160°C

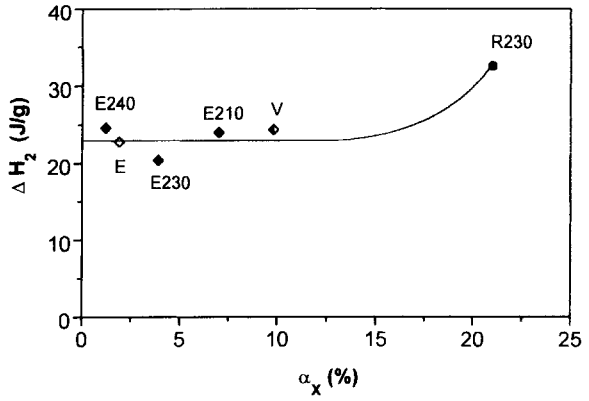

Figure 4 Melting heat ΔH_2 (measure of the crystallinity determined by d.s.c.) plotted against crystallinity index α_X (measure of the crystallinity determined by WAXS)

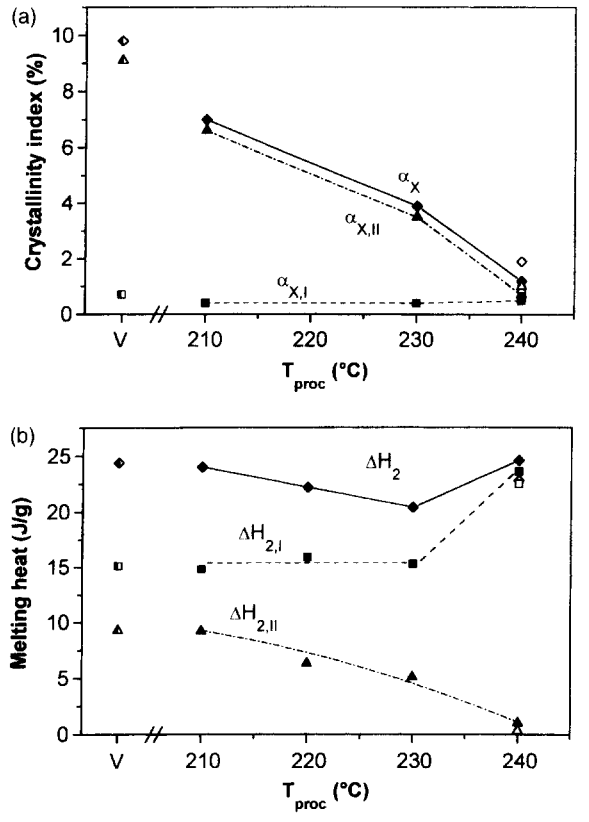

Figure 5 (a) Influence of processing temperature T_{proc} during injection moulding on the crystallinity index α_X and its parts $\alpha_{X,I}$, $\alpha_{X,II}$. Samples E210, E230, and E240, full symbols. For comparison: granule V, half full symbols; granule E, open symbols. (b) Influence of processing temperature T_{proc} during injection moulding on the melting heat ΔH_2 and its parts $\Delta H_{2,I}$, $\Delta H_{2,II}$. Samples E210–E240, full symbols. For comparison: granule V, half full symbols; granule E, open symbols

assumption that both methods detect the same overall crystallinity in the case of the sample R230. In *Figure 6* the related values obtained by WAXS are plotted in dependence on related values obtained by d.s.c. Analogously to the results shown above α_X and $\alpha_{X,II}$ give nearly the same behaviour. The line plotted in *Figure 6* was obtained on the supposition that $\Delta H_{2,II}$ represents the heat of fusion of all crystallites 'type II', determined by WAXS ($\alpha_{X,II}$). The experimental values show only small deviations from this line. This result confirms our hypothesis of the assignment of $\alpha_{X,II}$ to $\Delta H_{2,II}$.

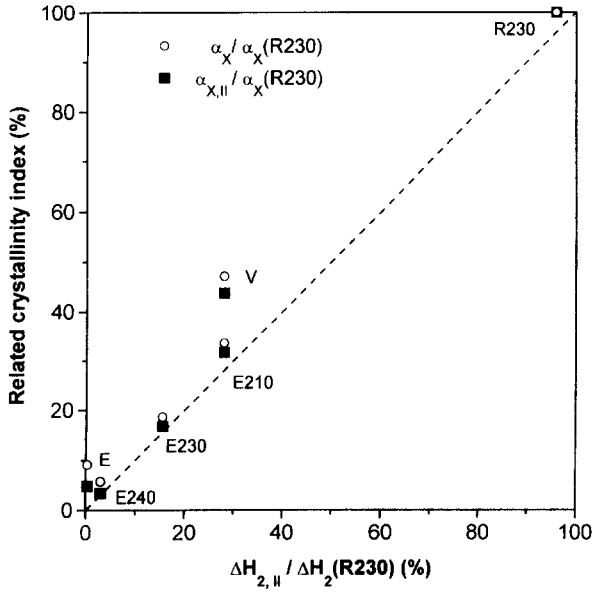

Figure 6 Ratio α_X/α_X(R230) and $\alpha_{X,II}/\alpha_X$(R230) as a function of the ratio $\Delta H_{2,II}/\Delta H_2$(R230) for all investigated samples

The strong influence of the processing temperature on the melting behaviour can be explained, if this temperature is compared to the melting temperature range of the used granules. In dependence on the chosen processing temperature, an annealing and/or melting of HS crystallites take place during processing. The increase of the content of HS crystallites 'type II' at low processing temperatures results from the annealing of the non-molten part of HS crystallites. Additionally, a recrystallization of the molten HS crystallites 'type I' into 'type II' is possible. At high processing temperatures (> 230°C) all HS crystallites melt completely, and the thermodynamically more stable crystallite 'type I' will be formed favourably by the crystallization of the melt after processing.

MECHANICAL PROPERTIES

The glass transition temperature $T_{g,ss}$ of the soft segment phase and some mechanical properties of the TPU samples E2XX are given in *Table 5*. Additionally, the mechanical properties of the samples V210 and V240[a], prepared from virgin granules V, are listed.

The lowest values of glass transition temperature $T_{g,ss}$ and tensile strength were observed at sample E210. From further investigations we know that the stronger phase separation, characterised by a decrease of glass transition temperature $T_{g,ss}$, is connected with the presence of HS crystallites with higher melting temperatures. According to the results presented in this paper, these HS crystallites have the morphology of 'type II'. The results discussed above show that the formation of HS crystallites 'type II' is apparently connected with a stronger phase separation, whereas the dominant presence of 'type I' is connected with a higher degree of phase mixing.

In *Figure 7* the tensile strength is plotted in dependence on the ratio $\Delta H_{2,I}/\Delta H_2$. At $\Delta H_{2,I}/\Delta H_2 \approx 80\%$ a weak maximum in tensile strength can be observed. This result shows that a special overall morphology is necessary for optimal mechanical properties. Seymor and Cooper[6] assumed that the phase separation is responsible for the mechanical properties. It is not clear yet, whether the main influence on the tensile strength is the morphology of the HS

Table 5 Glass transition temperatures of TPU soft segments $T_{g,ss}$ and tensile properties of injection moulded samples

Sample	$T_{g,ss}$ (°C)	Tensile strength, σ_b (MPa)	Elongation at break, ε_b (%)
V210		43.9	285
V240		56.4	375
E210	21.6	45.5	267
E220	23.2	50.6	314
E230	22.5	55.4	351
E240	23.8	54.7	355

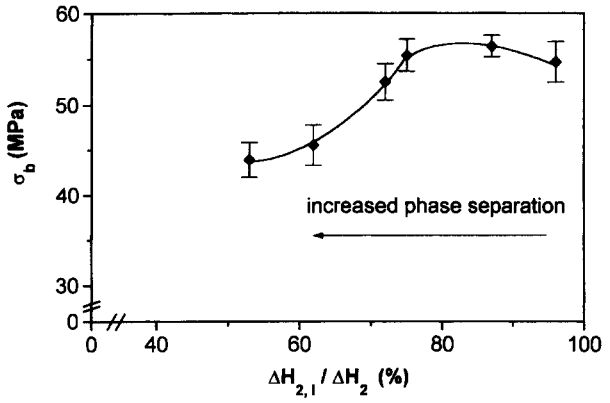

Figure 7 Tensile strength σ_b in dependence on the ratio $\Delta H_{2,I}/\Delta H_2$

crystallites or the degree of phase separation, because both effects are correlated with each other. The dependence shown in *Figure 7* supports the hypothesis that the interpretation of the structure–property relationship should be based rather on crystallite morphology[6]. Beyond this, the observed behaviour allows to establish a processing–structure–property relationship. The content of crystallites of 'type I' and 'type II' as well as the overall phase separation can be controlled just by varying the processing temperature. With known melting behaviour of the used granules, the chosen processing temperature determines the content of crystallites 'type I' and 'type II' of the produced specimens. In this way, it is possible to choose processing conditions which result in a morphology corresponding to good mechanical properties. This result is one step in the field of controlled processing of polyurethane.

SUMMARY

The resulting phase morphology of thermoplastic polyurethane elastomers depends on the processing conditions.

In the TPU studied in this paper two different morphologies of the MDI/BD-based HS crystallites were visible. While the overall crystallinity of TPU is almost independent of the conditions during injection moulding, the content of the different crystallite types strongly depends on the maximum processing temperature. If processing takes place below 230°C, a high content of crystallites of 'type II' is observed formed by melting and recrystallization of 'type I' crystallites during processing. The melting temperature T_m is $\geq$ 220°C, whereby the main peak is at about 230°C.

Processing at higher temperatures results in the thermodynamically more stable 'type I' crystallites with $T_m \leq$ 220°C, whereby the main peak is at about 210°C. These crystallites were formed favourably during the relatively fast cooling of the melt in the mould and also during cooling in the d.s.c. at 10 K/min.

The assignment of the two different crystallite types to the different melting regions is possible by comparing the d.s.c. melting behaviour with the WAXS results. The crystallinity, determined by means of WAXS is characterized mainly by the crystallinity caused by 'type II' crystallites, which show strong and weak reflection. The main reflection is at 0.463 nm. The intensity of the WAXS pattern of 'type I' crystallites is very weak and broad. This shows that the crystallites of 'type II' are highly ordered and have a relatively big size in comparison to the crystallites of 'type I', the size of which should be smaller than 7 nm.

The mechanical strength of the TPU is directly correlated to the phase morphology. Apparently, for high tensile strength a certain degree of phase separation, which corresponds to a certain composition of 'type I' and 'type II' crystallites, is necessary. This morphology can be reached by choosing proper processing conditions, considering the melting behaviour of the used virgin granules in respect to the different melting behaviour of both crystalline structures.

REFERENCES

1. Gibson, P. E., Vallance, M. A. and Cooper, S. L., in *Development in Block Copolymers*, ed. I. Goodman, Applied Science Series, Elsevier, London, 1982, p. 217.
2. Cooper, S. L. and Tobolsky, A. V., *J. Appl. Polym. Sci.*, 1966, **10**, 1837.
3. Van Bogart, J. W. C., Gibson, P. E. and Cooper, S. L., *J. Polym. Sci., Polym. Phys.*, 1983, **21**, 65.
4. Harris, R. F., Joseph, M. D., Davidson, C., De Porter, C. D. and Dais, V. A., *Polymer Preprints*, 1989, **30**, 235.
5. Li, Y., Gao, T., Liu, J., Linliu, K., Desper, C. R. and Chu, B., *Macromolecules*, 1992, **25**, 7365.
6. Seymour, R. W. and Cooper, S. L., *Macromolecules*, 1973, **6**, 48.
7. Pohl, G., Joel, D., Goering, H. and Carius, H.-E., *Plaste und Kautschuk*, 1993, **40**, 357.
8. Li, Y., Gao, T. and Chu, B., *Macromolecules*, 1992, **25**, 1737.
9. Leung, L. M. and Koberstein, J. T., *Macromolecules*, 1986, **19**, 706.
10. Bonart, R., Morbitzer, L. and Hentze, G., *J. Macromol. Sci.-Phys.*, 1969, **B3**(2), 337.
11. Blackwell, J., Nagarajan, M. R. and Hoitink, T. B., *Polymer*, 1982, **23**, 950.
12. Blackwell, J. and Lee, C. D., *J. Polym. Sci., Polym. Phys.*, 1984, **22**, 759.
13. Briber, R. M. and Thomas, E. L., *J. Macromol. Sci.-Phys.*, 1983, **B22**, 509.
14. Koberstein, J. T. and Russell, T. P., *Macromolecules*, 1986, **19**, 714.
15. Koberstein, J. T. and Galambos, A. F., *Macromolecules*, 1992, **25**, 5618.
16. Samuels, S. L. and Wilkes, G. L., *J. Polym. Sci., Polym. Phys.*, 1973, **11**, 807.
17. Briber, R. M. and Thomas, E. L., *J. Polym. Sci., Polym. Phys.*, 1985, **23**, 1915.
18. Born, L., Crone, J., Hespe, H., Müller, R. H. and Wolf, K. H., *J. Polym. Sci., Polym. Phys.*, 1984, **22**, 163.